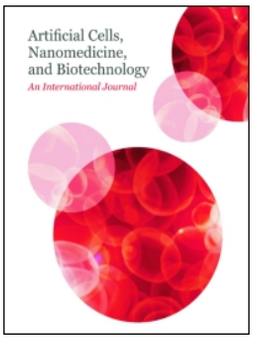

Taylor & Francis
Taylor & Francis Group

Artificial Cells, Nanomedicine, and Biotechnology
An International Journal

ISSN: 2169-1401 (Print) 2169-141X (Online) Journal homepage: informahealthcare.com/journals/ianb20

Ciprofloxacin HCl-loaded calcium carbonate nanoparticles: preparation, solid state characterization, and evaluation of antimicrobial effect against *Staphylococcus aureus*

Solmaz Maleki Dizaj, Farzaneh Lotfipour, Mohammad Barzegar-Jalali, Mohammad-Hossein Zarrintan & Khosro Adibkia

To cite this article: Solmaz Maleki Dizaj, Farzaneh Lotfipour, Mohammad Barzegar-Jalali, Mohammad-Hossein Zarrintan & Khosro Adibkia (2017) Ciprofloxacin HCl-loaded calcium carbonate nanoparticles: preparation, solid state characterization, and evaluation of antimicrobial effect against *Staphylococcus aureus*, Artificial Cells, Nanomedicine, and Biotechnology, 45:3, 535-543, DOI: 10.3109/21691401.2016.1161637

To link to this article: https://doi.org/10.3109/21691401.2016.1161637

Published online: 25 Mar 2016.

Submit your article to this journal

Article views: 3382

View related articles

View Crossmark data

Citing articles: 21 View citing articles

Full Terms & Conditions of access and use can be found at
https://informahealthcare.com/action/journalInformation?journalCode=ianb20

ARTIFICIAL CELLS, NANOMEDICINE, AND BIOTECHNOLOGY, 2017
VOL. 45, NO. 3, 535–543
http://dx.doi.org/10.3109/21691401.2016.1161637

Taylor & Francis
Taylor & Francis Group

Ciprofloxacin HCl-loaded calcium carbonate nanoparticles: preparation, solid state characterization, and evaluation of antimicrobial effect against *Staphylococcus aureus*

Solmaz Maleki Dizaj[a,b], Farzaneh Lotfipour[c,d], Mohammad Barzegar-Jalali[d], Mohammad-Hossein Zarrintan[d] and Khosro Adibkia[d]

[a]Research Center for Pharmaceutical Nanotechnology, Tabriz University of Medical Sciences, Tabriz, Iran; [b]Student Research Committee, Tabriz University of Medical Sciences, Tabriz, Iran; [c]Hematology and Oncology Research Center, Tabriz University of Medical Sciences, Tabriz, Iran; [d]Faculty of Pharmacy, Drug Applied Research Center, Tabriz University of Medical Sciences, Tabriz, Iran

ABSTRACT

Ciprofloxacin HCl-loaded calcium carbonate ($CaCO_3$) nanoparticles were prepared via a w/o *microemulsion* method and characterized by dynamic light scattering, scanning electron microscopy, X-ray powder diffraction (XRPD) analysis, differential scanning calorimetry (DSC), and Fourier transform infrared spectroscopy (FTIR). The *in vitro* drug release profiles as well as antimicrobial effect against *Staphylococcus aureus* (*S. aureus*) were also evaluated. The antibacterial effect was studied using serial dilution technique to determine the minimum inhibitory concentration (MIC) of the nanoparticles and was confirmed by streak cultures. The mean particle size, drug loading and entrapment efficiency were calculated to be 116.09 nm, 20.49% and 44.05%, respectively. PXRD and FTIR studies confirmed that both vaterite and calcite polymorphs of $CaCO_3$ were formed during the preparation process. *In vitro* release profiles of the nanoparticles showed slow release pattern for 12 h. The drug-loaded nanoparticles showed similar MICs against *S. aureus* compared to untreated drug. However, a preserved antimicrobial effect was observed for drug-loaded nanoparticles compared to untreated drug after 2 days of incubation.

ARTICLE HISTORY
Received 22 November 2015
Revised 29 February 2016
Accepted 29 February 2016
Published online 24 March 2016

KEYWORDS
Antimicrobial activity; $CaCO_3$; ciprofloxacin HCl; microemulsion; nanoparticles; *Staphylococcus aureus*

Introduction

Despite the recent progresses in antibiotic treatment and operation techniques, treatment of osteomyelitis, a bone infectious disease, is difficult and expensive. The conventional treatment of osteomyelitis is removal of the infected bone and adjacent soft tissue alongside the antibiotic treatment (Waldvogel et al. 1970). Systemic treatment of osteomyelitis needs high serum concentrations of antibiotics for a prolonged period of time and shows higher side effects (Uskoković and Desai 2014). Local delivery of the antibiotics may be a suitable alternative with better treatment efficiency, fewer side effects, low cost, and increased patient compliance (Benoit et al. 1998, Giamarellos-Bourboulis 2000, Gürsel et al. 2000, Korkusuz et al. 2001, Neut et al. 2003, Waldvogel et al. 1970). Depot antibiotic-loaded beads (Adams et al. 1992), cements (Solberg et al. 1999), and implantable antibiotic pumps (Perry et al. 1985) are the various methods of local administration of the antibiotics for the treatment of osteomyelitis. As a main problem, most of these local drug delivery systems are composed of non-resorbable matrices that need to be removed after the treatment. Therefore, a degradable carrier would have the great advantage of omitting the need for an additional surgery to remove the carrier (Benoit et al. 1998, Giamarellos-Bourboulis 2000, Gürsel et al. 2000, Korkusuz et al. 2001, Neut et al. 2003).

Recently, ultrafine pharmaceutical nanoparticles have demonstrated great advantage in terms of increasing the therapeutic efficacy and decreasing the side effects through concentrating the therapeutic agents on the desired sites in the body (Adibkia et al. 2012, 2011, Ahangari et al. 2013, Allahverdiyev et al. 2011, Dizaj et al. 2014, 2015b, 2015c). One of the most important inorganic minerals with a long history of application in the various medical fields is $CaCO_3$ that exists in three polymorphs of calcite, aragonite, and vaterite (Dizaj et al. 2015a, 2015b). Nanoparticles of $CaCO_3$ have been reported to be useful as a drug carrier for insulin (Haruta et al. 2003), betamethasone phosphate, erythropoietin, granulocyte-colony stimulating factor (G-CSF) (Ueno et al. 2005), validamycin (Qian et al. 2011), gentamicin sulfate (Dizaj et al. 2015b), and doxorubicin hydrochloride (Kamba et al. 2013). $CaCO_3$ has been identified to be bioresorbable, biodegradable, and osteoconductive (Dizaj et al. 2015a, Qian et al. 2011, Ueno et al. 2005). A delivery system composed of osteoconductive material can provide a suitable condition for the growth of damaged bone alongside antibiotic delivery purpose in the treatment of bone infectious disease like *osteomyelitis* (Biazar et al. 2015, Blokhuis et al. 2000, Eğri and Eczacıoğlu 2016). Lucas et al. (2001) developed gentamicin-integrated aragonite type of $CaCO_3$ materials for the dual applications of bone substitution and drug release.

Ciprofloxacin hydrochloride (HCl) is a synthetic broad-spectrum antibiotic, which belongs to the second generation of fluoroquinolones with the plasma half-life of 3–5 h (Jeong et al. 2008). It is active against both Gram-positive (such as

CONTACT Khosro Adibkia adibkia@tbzmed.ac.ir Faculty of Pharmacy, Tabriz University of Medical Sciences, Golgasht Street, Daneshgah Ave., Tabriz, Iran
© 2016 Informa UK Limited, trading as Taylor & Francis Group

Staphylococcus aureus) and Gram-negative (such as *Escherichia coli*) bacteria (Brunton 2011). Ciprofloxacin HCl acts by inhibiting DNA gyrase (topoisomerase II) and topoisomerase IV, the enzymes that are necessary for separating the bacterial DNA, thereby inhibiting the cell division (Drlica and Zhao 1997). Ciprofloxacin HCl has been beneficially administrated to eradicate various pathogens that cause common bone infectious diseases such as osteomyelitis (Jain et al. 2015, Koort et al. 2006).

Owing to the great potentials of $CaCO_3$ nanoparticles as drug delivery systems as well as the confirmed bone-related advantages of these materials, antibiotic-loaded $CaCO_3$ nanoparticles can open new prospects to the treatment of bone infections. The aim of the present work was to prepare ciprofloxacin HCl-loaded $CaCO_3$ nanoparticles using a reverse phase microemulsion system. Subsequently, the morphological properties together with the physicochemical characteristics of the fabricated nanoparticles were investigated. The antimicrobial effects against *S. aureus*, the *most* common microorganism involved in the *osteomyelitis, were assessed as well.*

Experimental

Materials

Ciprofloxacin HCl was supplied from Temad Co. (Tehran, Iran) and *S. aureus* in its lyophilized form was purchased from Institute of Pasture (Tehran, Iran). Cyclohexane, *n*-butyl alcohol, hexadecyl trimethyl ammonium bromide (CTAB), calcium chloride, and sodium carbonate were obtained from Merck Co. (Darmstadt, Germany).

Preparation of the ciprofloxacin HCl-loaded $CaCO_3$ nanoparticles

Reverse microemulsion method (w/o) was used to prepare ciprofloxacin HCl-loaded $CaCO_3$ nanoparticles (Qian et al. 2011). Briefly, 0.9 g of *n*-butyl alcohol and 1.65 g of cyclohexane were mixed and stirred. Then, 0.58 g of CTAB as the organic phase surfactant was added and the mixture was stirred at 400 rpm. Subsequently, 50 µl aqueous solution of $CaCl_2$ (5 M) and 50 µl aqueous solution of ciprofloxacin HCl (3 g/dl) were added into the mixture, and the microemulsion was formed after stirring at 1400 rpm for 20 min. Ciprofloxacin HCl-loaded $CaCO_3$ nanoparticles were precipitated by adding 50 µl of Na_2CO_3 (2 M) into the microemulsion system. The resulting microemulsion was maintained under a gentle mixing for 24 h to evaporate off the organic solvent. Finally, the prepared suspension was centrifuged (Eppendorf AG 5810R, Germany) in 12,000 rpm for 10 min to separate the nanoparticles. Nanoparticles were washed twice with 2 ml of distilled water and then 2 ml of methanol in the centrifuge tube. The blank $CaCO_3$ nanoparticles were also prepared with the same process (without drug). The physical mixture of ciprofloxacin HCl and the blank $CaCO_3$ nanoparticles was prepared taking into account of the drug-loading data (20.49%) by tumble mixing for 10 min.

Characterization of the nanoparticles

Particle size and morphology

The mean diameter of nanoparticles was obtained via Dynamic Light Scattering (DLS) technique (Malvern, United Kingdom) at 25 ± 1 °C. Moreover, SEM analysis (SEM, TESCAN, Warrendale, PA) was applied to study the morphology and structure of both the $CaCO_3$ nanoparticles and ciprofloxacin HCl-loaded $CaCO_3$ nanoparticles. The dry *powder of nanoparticles* was sputter-coated with gold before examination.

The drug loading and entrapment efficiency

To determine the entrapment efficiency, 100 mg of the prepared ciprofloxacin HCl-loaded $CaCO_3$ nanoparticles was dissolved in EDTA (0.5 M, pH 7.5) (Qian et al. 2011, Ueno et al. 2005). The mixture was stirred magnetically for 30 min and then 1 ml of water phase was taken to measure drug loading efficiency. Absorbance of aqueous phase was measured at 277 nm using UV–visible spectrophotometer (UV1800 Shimadzu, Kyoto, Japan). Afterwards, using the previously prepared standard curve (linear in the range of 2–32 mcg/ml, $y = 0.0379x - 0.0154$, $R^2 = 0.9998$), the percent of drug loading and entrapment efficiency were calculated according to the following equations:

$$\text{Drug loading } (\%) = (\text{drug content/total amount (weight) of obtained nanoparticles}) \times 100$$

$$\text{Entrapment efficiency } (\%) = (\text{drug content/total drug added}) \times 100$$

Zeta potential measurements

Zeta potential measurements were performed to get information about the surface charge of the nanoparticles. Zeta potential of the prepared nanoparticles was measured using zeta-sizer (Malvern, UK) at 25 ± 1 °C. The freshly prepared suspension was diluted with distilled water and injected into the capillary cell of zeta-sizer.

Powder X-ray diffraction (PXRD) analysis

PXRD patterns were recorded at room temperature for ciprofloxacin HCl, $CaCO_3$ nanoparticles, physical mixture of ciprofloxacin HCl, and $CaCO_3$ nanoparticles as well as ciprofloxacin HCl-loaded $CaCO_3$ nanoparticles using an X-ray diffractometer (Siemens, Model D5000, Germany) operating with Cu Kα radiation of wavelength 1.5405 Å, a voltage of 40 kV, and a current of 30 mA.

Differential scanning calorimetry (DSC) analysis

DSC analysis of the prepared formulations was performed to determine any changes in the thermal behavior of the drug during the preparation of nanoparticle using DSC60 (Shimadzu, Japan). The accurately weighed samples of 5 mg were placed

into the aluminum pans and sealed. The instrument temperature was calibrated using the aluminum oxide and indium powders as a reference and a standard, respectively. A heating rate of 40 °C/min from 30 to 350 °C was applied for recording of spectra. The obtained thermograms were analyzed using TA60 software.

Fourier transform infrared spectroscopy (FTIR) analysis

FTIR spectra were recorded to confirm the chemical structures of ciprofloxacin HCl and $CaCO_3$ nanoparticles and to evaluate any probable drug/carrier interaction in the prepared formulation. FTIR patterns for ciprofloxacin HCl, $CaCO_3$ nanoparticles, and physical mixture of ciprofloxacin HCl and $CaCO_3$ nanoparticles as well as ciprofloxacin HCl-loaded $CaCO_3$ nanoparticles were obtained using an FTIR spectrophotometer (Shimadzu 43000, Kyoto, Japan) via the KBr disk method from 4000 to 400 cm^{-1} at a resolution of 4 cm^{-1}.

In vitro *drug release*

In vitro drug release study for the prepared formulations was performed using a USP apparatus II, paddle stirrer, and 300 ml buffer phosphate (pH = 7.4) was used as a dissolution medium. All dissolution experiments were performed under orbital mixing (50 rpm) at 37 °C. At specified times, 3 ml of medium was withdrawn and filtered through cellulose acetate membrane (Whatman, Kent, UK) with pore diameter of 20 nm and replaced by 3 ml fresh buffer phosphate (pH = 7.4). The concentration of released drug was measured with a UV–visible spectrophotometer (UV-1601 PC; Shimadzu, Kyoto, Japan) at 272 nm. Release profiles were plotted for pure ciprofloxacin HCl, $CaCO_3$ nanoparticles, physical mixture of ciprofloxacin HCl, and $CaCO_3$ nanoparticles as well as ciprofloxacin HCl-loaded $CaCO_3$ nanoparticles.

To find out the drug release mechanism, the *in vitro* release data were fitted to 10 common kinetic models including zero-order, first-order, Higuchi, Pepas, Hixon-Crowell, square root of mass, three seconds root of mass, Weibull, Linear probability, and Log probability models (Barzegar-Jalali 1990, Barzegar-Jalali et al. 2010). The accuracy and prediction ability of the models were compared by calculation of squared correlation coefficients (*RSQ*) and percent error (*PE*) (Barzegar-Jalali et al. 2008).

Preparation of the drug stock solution

For preparing the drug stock solution, 256 mg of ciprofloxacin HCl powder was accurately weighed and dissolved in the 10 ml of prepared buffer (USP No. 3). For preparing the buffer, monobasic potassium phosphate (0.523 g) and dibasic potassium phosphate (16.73 g) were dissolved in distilled water (1000 ml) and the pH of solution was adjusted to 8.0 ± 0.1.

Inoculum preparation

The standard *S. aureus* was activated according to the provider protocol and the cultures of bacteria were maintained in their proper agar media at 4 °C throughout the study as the stock cultures. Briefly, a single colony from the stock cultures was transferred into Mueller Hinton Broth and incubated overnight (37 °C). The incubated cells were collected by centrifugation at 3000 rpm for 10 min. Then, to provide a bacterial concentration around 10^8 CFU/ml, collected cells were washed twice and re-suspended in saline solution. Finally, the concentration of inoculum was adjusted to approximately 10^6 CFU/ml with sterile saline solution.

Determination of minimum inhibitory concentrations (MICs)

MICs were determined using broth macro-dilution MIC method. Briefly, twofold serial dilutions of ciprofloxacin HCl were prepared using sterile buffer (USP No. 3) in the concentration ranges of 0.5–128 μg/l. Then, 100 μl of bacterial inocula was transferred into the tubes and all tubes were incubated for 24 h (35 °C). After 24 h, the content of the tubes was streak-cultured onto Mueller-Hinton agar plates. The first concentration with no sign of bacterial growth on the plates was considered as MIC. MIC processes were also carried out for $CaCO_3$ nanoparticles, physical mixture of ciprofloxacin HCl, and $CaCO_3$ nanoparticles as well as ciprofloxacin HCl-loaded $CaCO_3$ nanoparticles.

Results and discussion

Particle size and morphology

Particle size distributions of the blank and drug-loaded $CaCO_3$ nanoparticles are shown in Figure 1. The average diameters of the blank $CaCO_3$ nanoparticles and ciprofloxacin HCl-loaded $CaCO_3$ nanoparticles were 89.64 nm and 116.09 nm, respectively. The particle size distributions were relatively monodisperse in both formulations with the polydispersity index (*PDI*) values of 0.246 and 0.216 for the blank $CaCO_3$ nanoparticles and drug-loaded $CaCO_3$ nanoparticles, respectively (Adibkia et al. 2012, Jana et al. 2014). The diameters obtained by the

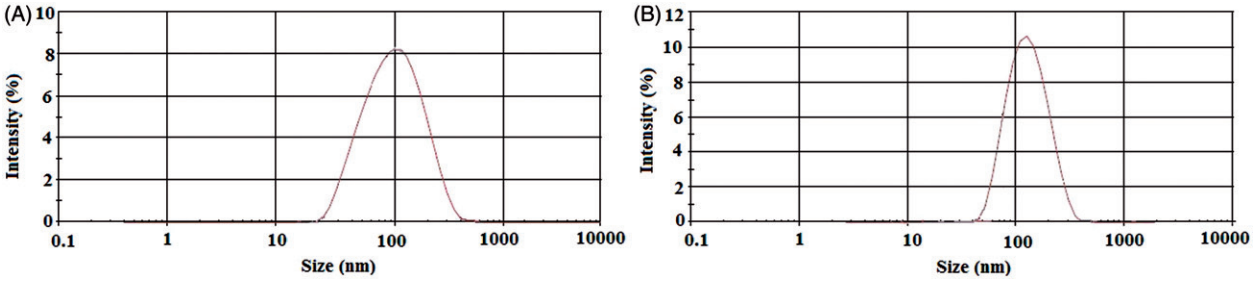

Figure 1. Particle size distribution of the prepared nanoparticles: (A) blank $CaCO_3$ nanoparticles and (B) ciprofloxacin HCl-loaded $CaCO_3$ nanoparticles.

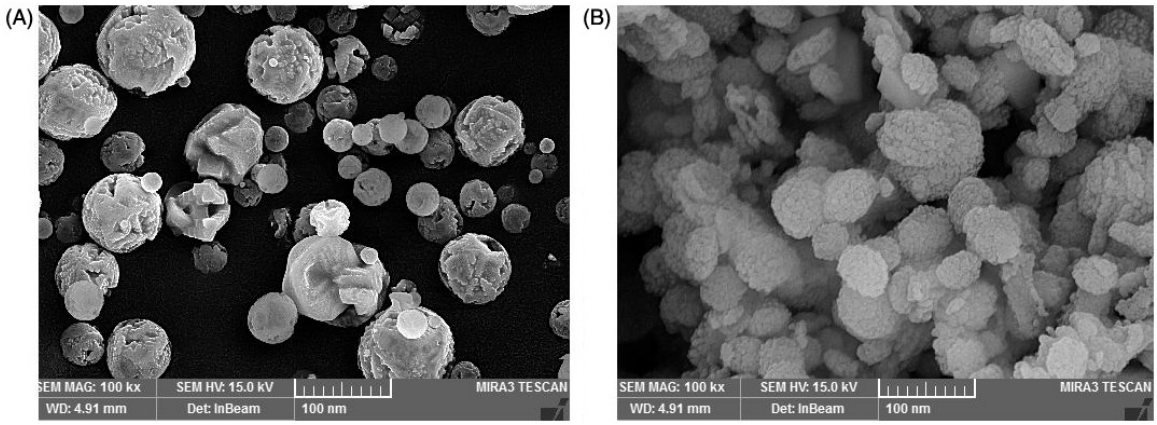

Figure 2. SEM images of the prepared nanoparticles: (A) blank $CaCO_3$ nanoparticles and (B) ciprofloxacin HCl-loaded $CaCO_3$ nanoparticles.

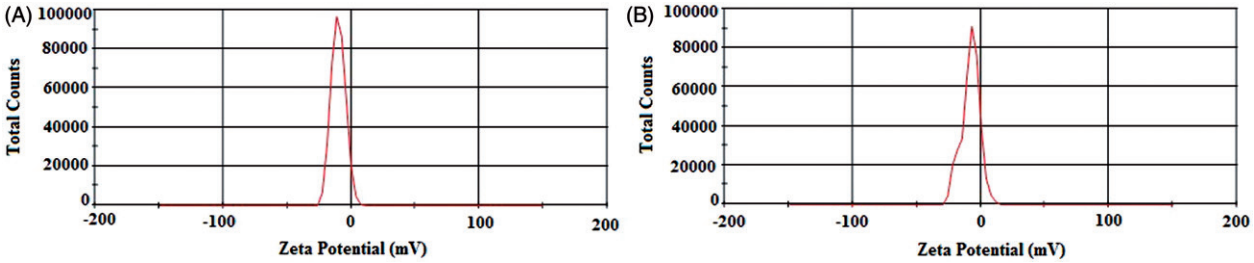

Figure 3. Zeta potential of the prepared nanoparticles: (A) blank $CaCO_3$ nanoparticles and (B) ciprofloxacin HCl-loaded $CaCO_3$ nanoparticles.

DLS for the prepared nanoparticles were larger than the size observed by the SEM. It might be occurred due to an error in the Stokes–Einstein equation for DLS technique (for viscosity magnitudes) (Berne and Pecora 2000). Other investigators have reported similar results for drug-loaded nanoparticles (Darvishi et al. 2014, Mo and Lim 2005).

Calcite polymorph of $CaCO_3$ exists in the forms of rhombohedral, truncated prismatic, scalenohedral, spherical, or chain-like agglomerates (Ukrainczyk et al. 2009), while vaterite and aragonite polymorphs exist mainly in cauliflower-like and needle-like forms, respectively (Andreassen 2005). Based on SEM analysis of the prepared nanoparticles (Figure 2), crystal structure of the blank $CaCO_3$ nanoparticles was mainly spherical calcite, while the cauliflower-like vaterite was prevalent morphology of ciprofloxacin HCl-loaded $CaCO_3$ nanoparticles (Kirboga and Oner 2013, Ukrainczyk et al. 2007).

The drug loading and entrapment efficiency

The drug loading and entrapment efficiency, important factors for a drug delivery system, are used to evaluate the usability of nano-based carriers (Kamba et al. 2013). Entrapment efficiency and the drug loading of the ciprofloxacin HCl in $CaCO_3$ nanoparticles were calculated to be $44.05 \pm 1.68\%$ and 20.49 ± 0.09, respectively. A reverse phase microemulsion method (w/o) using *n*-butyl alcohol and cyclohexane as binary organic phase can provide proper entrapment efficiency for the hydrophilic drugs such as ciprofloxacin HCl, due to their insolubility in organic nature of the external phase (Montaseri et al. 2010, Sah and Sah 2015). Qian et al. (2011) used similar method for entrapment of validamycin, water-soluble antibiotic, into $CaCO_3$ nanoparticles with entrapment efficiency of 19.3%.

Zeta potential measurements

Zeta potential gives information on the surface charge of the prepared nanoparticles. Zeta potential value is an important parameter for predicting the stability of the nanoparticles as well as their interaction with the biological environment such as cellular uptake by macrophages (Vogelman et al. 1988). Figure 3 shows the values of the zeta potential for the blank and drug-loaded $CaCO_3$ nanoparticles. The blank and drug-loaded $CaCO_3$ had zeta potential values of -9.95 mV and -9.90 mV, respectively.

It has been proposed that negative values of the zeta potential have an important favorable effect on the attachment and proliferation of the bone cells (Cooper and Hunt 2006). Several studies on the zeta potential of synthetic bioceramics like hydroxyapatite and other calcium derivatives (Cooper and Hunt 2006, Smeets et al. 2009, Teng et al. 2001) have revealed that a negative zeta potential value could improve the *in vivo* biological effects (Smeets et al. 2009). According to a number of studies, a material with negative zeta potential is more available for the attachment and proliferation of osteoblasts than neutral or positive surfaces (Teng et al. 2001). Considering that the nanoparticles with a zeta potential between -10 and -30 mV are considered negatively charged particles (Clogston and Patri 2011), so therefore, the prepared nanoparticles in the present study with zeta potential of about -10 mV might be superiorly attached to the osteoblasts.

In vitro release profiles of the drugs can also be influenced by zeta potential of the nanoparticles (Honary and Zahir 2013). Furthermore, the surface charge of the particles is the important parameter that controls the drug loading efficiency. The zeta potential can also be used to determine whether an active material (such as drug) is incorporated within or

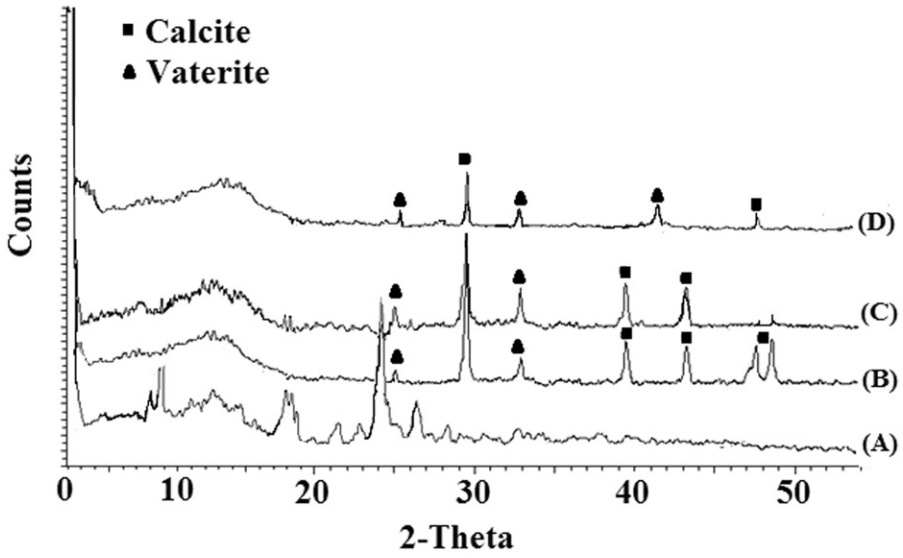

Figure 4. XRPD patterns of (A) pure ciprofloxacin HCl, (B) $CaCO_3$ nanoparticles, (C) physical mixture of ciprofloxacin HCl and $CaCO_3$ nanoparticles and (D) ciprofloxacin HCl-loaded $CaCO_3$ nanoparticles.

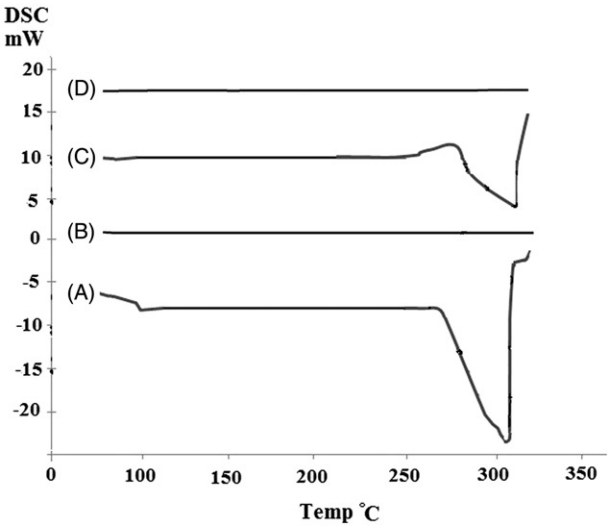

Figure 5. DSC thermograms of (A) pure ciprofloxacin HCl, (B) $CaCO_3$ nanoparticles, (C) physical mixture ciprofloxacin HCl and $CaCO_3$ nanoparticles and (D) ciprofloxacin HCl-loaded $CaCO_3$ nanoparticles.

adsorbed on the surface of the nanoparticle (Honary and Zahir 2013, Honary et al. 2010). The presence of ciprofloxacin HCl did not influence the zeta potential of the drug-loaded $CaCO_3$ nanoparticles compared to the blank $CaCO_3$ nanoparticles, which might be due to the fact that the drug was uniformly entrapped within the nanoparticles (Dillen et al. 2006).

PXRD analysis

The crystallinity of ciprofloxacin HCl in the drug-loaded nanoparticles was investigated by X-ray diffraction (Figure 4). The X-ray diffraction pattern of the ciprofloxacin HCl powder demonstrated the presence of the characteristic bands showing its crystalline nature (Mobarak et al. 2014) (Figure 4, curve A). PXRD analysis also confirmed the existence of mixture of calcite and vaterite polymorphs for both blank and drug-loaded $CaCO_3$ nanoparticles (Kirboga and Oner 2013). The characteristic peaks of calcite polymorph appeared at 2θ of 29.4°, 39.5°, 43.0°, and 48° (Ni and Ratner 2008, Shen et al. 2007), while the diffraction peaks at 24.92°, 42, 32.78°, and 50.0° were related to vaterite polymorph (Kirboga and Oner 2013, Tai and Chen 2008). Chen and Xiang (2009) and Wang et al. (2010) reported similar observations for simultaneous formation of $CaCO_3$ polymorphs. Curve D (in Figure 4) shows the X-ray diffraction of drug-loaded $CaCO_3$ nanoparticles where the drug bands were completely disappeared indicating the entrapment of an amorphous drug into the $CaCO_3$ matrix (Mobarak et al. 2014). Similar results have been reported by Mobarak et al. (2014) and Jeong et al. (2008) for ciprofloxacin HCl-loaded polymeric nanoparticles.

DSC analysis

DSC curves provided information on the thermal behavior of the drug in the prepared formulations (Figure 5). Ciprofloxacin HCl (Figure 5, curve A) was characterized by an endothermic peak at 303 °C, corresponding to its melting point (Mobarak et al. 2014). The range of melting point for different polymorphs of $CaCO_3$ is between 825 °C and 1339 °C (Qian et al. 2011). Then, $CaCO_3$ blank nanoparticles did not exhibit any peak up to 350 °C (Figure 5, curve B). The curve related to physical mixture of ciprofloxacin HCl and $CaCO_3$ nanoparticles also showed the melting peak of the drug at 308 °C (Figure 5, curve C). Lower intensity of the melting peak in the physical mixture might be related to the dilution effect of carrier (Jahangiri et al. 2014). The characteristic peak of the drug was disappeared in the thermogram of drug-loaded nanoparticles (Figure 5, curve D). It could be concluded that ciprofloxacin HCl was entrapped in an amorphous form into the $CaCO_3$ matrix. Such an observation has also been reported by other investigators (Cevher et al. 2007, Dillen et al. 2004, Mobarak et al. 2014).

FTIR analysis

The FTIR peaks of the pure ciprofloxacin HCl, $CaCO_3$ nanoparticles, physical mixture of ciprofloxacin HCl, and $CaCO_3$

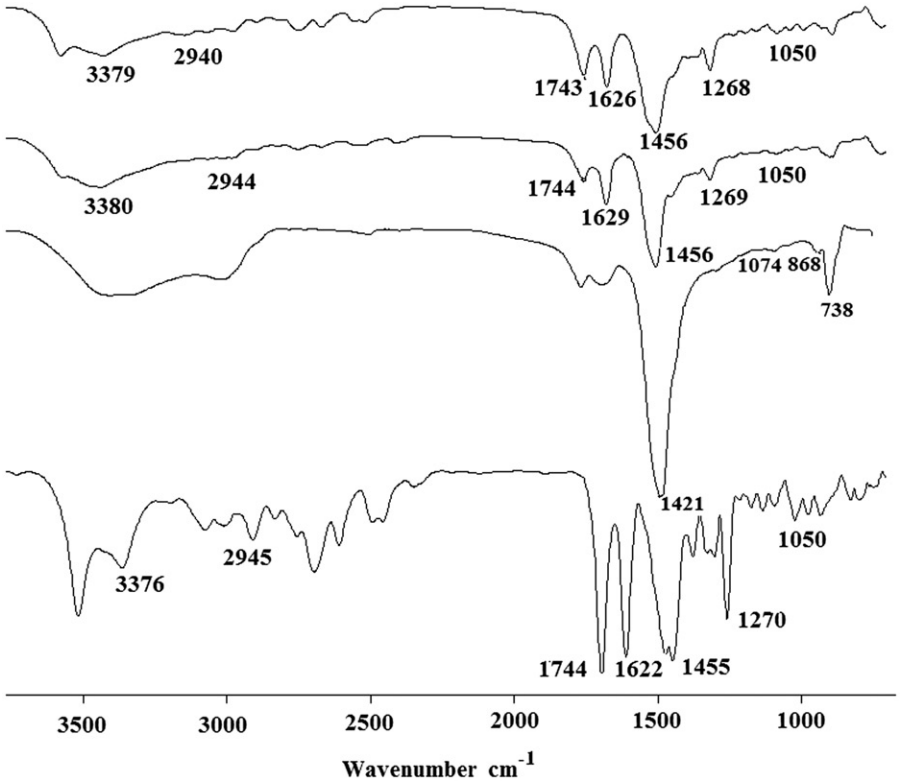

Figure 6. FTIR spectra of (A) pure ciprofloxacin HCl, (B) $CaCO_3$ nanoparticles, (C) physical mixture of ciprofloxacin HCl and $CaCO_3$ nanoparticles and (D) ciprofloxacin HCl-loaded $CaCO_3$ nanoparticles.

nanoparticles as well as ciprofloxacin HCl-loaded $CaCO_3$ nanoparticles are presented in Figure 6. In the FTIR spectra of ciprofloxacin HCl (Figure 6, curve A), a peak at 1050 cm^{-1} was assigned to C–F group and another characteristic peak at 1650 cm^{-1} was related to quinolones (Sahoo et al. 2011). The peak at the 1455 cm^{-1} was related to C–O and the bands at 1270 cm^{-1} was attributed to vibration of the O–H group related to the presence of carboxylic acid (Sahoo et al. 2011). A band at 2945 cm^{-1} indicated alkenes and aromatic C–H stretching and the bands at 1744 cm^{-1} signified carbonyl stretching (C=O) (Silverstein et al. 2014). A characteristic peak at 3376 cm^{-1} was related to the OH stretching vibration (Silverstein et al. 2014). In the curve B (in Figure 6), blank $CaCO_3$ nanoparticles exhibited the characteristic absorption peaks of CO_3^{2-} at 1421 cm^{-1} and 868 cm^{-1} related to the vibrations of calcite polymorph of $CaCO_3$ and the peak of CO_3^{2-} at 1074 cm^{-1} revealed vaterite polymorph of $CaCO_3$ (Kirboga and Oner 2013). The FTIR spectrum for the physical mixture of the drug and $CaCO_3$ nanoparticles (Figure 6, curve C) showed all characteristic peaks of the drug and $CaCO_3$ nanoparticles. The spectra of the drug-loaded nanoparticles (Figure 6, curve D) showed characteristic peaks of ciprofloxacin HCl (Sahoo et al. 2011) together with the peaks related to CO_3^{2-} of the calcite polymorph as well as the peak signified to $CO_3^{2-}$of the vaterite polymorph (Kirboga and Oner 2013). Absence of any significant change in position of the peaks of ciprofloxacin HCl in the drug-loaded nanoparticles indicated that there was no significant interaction between the drug and $CaCO_3$ during nanoparticles preparation process (Kumar et al. 2012, Mobarak et al. 2014).

In vitro *drug release*

Dissolution testing is a valuable tool to determine the amount of released drug from a solid form under known conditions of dissolution medium and time (Beyssac and Lavigne 2005, Jahangiri et al. 2014). Figure 7 shows the release patterns of pure ciprofloxacin HCl, physical mixture of ciprofloxacin HCl, and $CaCO_3$ nanoparticles as well as ciprofloxacin HCl-loaded $CaCO_3$ nanoparticles. The drug release from nanoparticles was more sustained than that of the pure drug, while the physical mixture showed a comparable drug release with the pure drug. The pure ciprofloxacin HCl was released in the first two hours, whereas the drug release from the nanoparticles was prolonged up to 12 h. Similarly, in the study by Ueno et al. (2005), G-CSF and betamethasone phosphate showed a significant sustained release profile from $CaCO_3$ nanoparticles. The sustained release profile of the drug from $CaCO_3$ nanoparticles have also been reported for validamycin (Qian et al. 2011) and insulin (Haruta et al. 2003).

The *in vitro* release data were fitted into 10 common kinetic models. Considering the *RSQ* of 0.99 and *PE* of 3.38%, the drug release data were best fitted to the Higuchi model. Higuchi's kinetic model can be used to describe the drug release from different kinds of modified release dosage forms (Kadivar et al. 2015). This model explains the release of drugs from insoluble matrix as a square root of time-dependent process based on Fickian diffusion equation (Kalam et al. 2007, Ofoefule and Chukwu 2002). Modeling of the drug release from the ciprofloxacin-Eudragit nanoparticles has also been described by Dillen et al. (2006) whose work showed that the release data were fitted to the Higuchi's kinetic model.

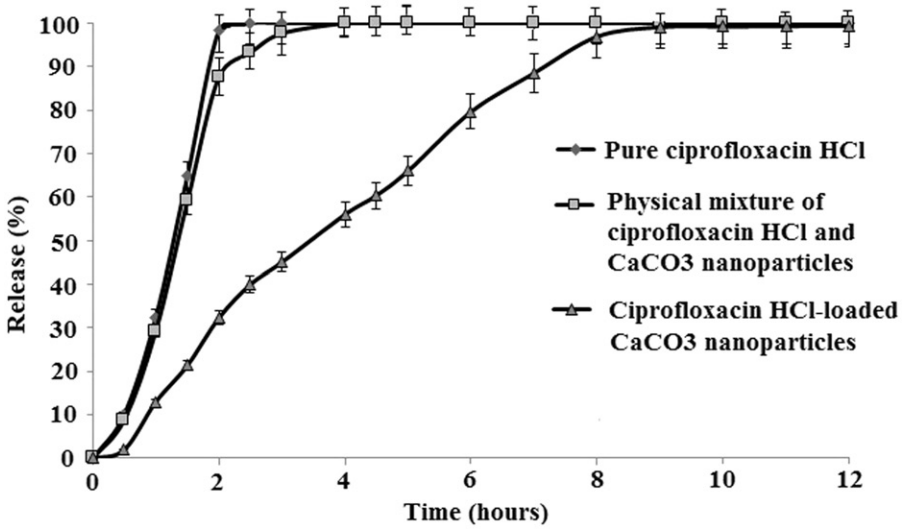

Figure 7. Drug release profile for ciprofloxacin HCl, physical mixture of ciprofloxacin HCl and $CaCO_3$ nanoparticles, and ciprofloxacin HCl-loaded $CaCO_3$ nanoparticles. Each point is the average of three replications and the vertical bars represent standard deviations.

Antimicrobial efficiency

Based on the results of antimicrobial testing experiments, ciprofloxacin HCl-loaded $CaCO_3$ nanoparticles maintained its antimicrobial effectiveness with equal MIC values to untreated ciprofloxacin HCl against test organism of *S. aureus* (1 μg/ml). Similar findings were obtained in a research by Dillen *et al.* with no significant differences in the MIC values of ciprooxacin-loaded Eudragit/PLGA nanoparticles and untreated ciprofloxacin (Dillen et al. 2006). Furthermore, physical mixture of ciprofloxacin HCl and $CaCO_3$ nanoparticles showed an equal antimicrobial activity to the drug solution.

The equal MICs for untreated ciprofloxacin HCl solution and ciprofloxacin HCl-loaded $CaCO_3$ nanoparticles suggested effective entrapment of the drug into the $CaCO_3$ nanoparticles without losing its pharmacological effect. The blank nanoparticles exhibited no antibacterial effect signifying the inert nature of $CaCO_3$ nanoparticles. So therefore, hopeful features of $CaCO_3$ nanoparticles as a drug carrier can be advantageously applied in delivery of ciprofloxacin HCl.

Interestingly, a decrease in the growth extent of *S. aureus* after two days incubation of the streak cultures was observed for the drug-loaded $CaCO_3$ nanoparticles compared to that of untreated drug solution. It can be assumable that the sustained released features of $CaCO_3$ nanoparticles adsorbed to the cell surface of the microorganisms can act as a drug depot to decline the growth rate of the bacteria. Such a result has been presented by Kesavan *et al.* for gatifloxacin gellan system against *S. aureus* (Kesavan et al. 2010). Validamycin-loaded $CaCO_3$ nanoparticles also presented a preserved antimicrobial activity against *Rhizoctonia solani* in a study by Qian et al. (2011).

There are some suggested mechanisms that dominantly facilitate the penetration of drug content of the nanocarrier into the bacterial cells and therefore deliver the drug into its site of action in an improved manner (Esmaeili et al. 2007). Nanoparticles can fuse with the bacterial cell wall and subsequently the drug is released across the cell wall and cell membrane. Adsorption of the nanoparticles to the bacterial cell wall can be another mechanism which provides a sustained antimicrobial activity of the incorporated antibiotic against the microorganisms (Darvishi et al. 2014, Zhang et al. 2010). Antibiotic-loaded nanoparticles can also attract to the infection site and not only release the drug at the infection site but also, after phagocytosis of the pathogen, expose it to the high intracellular drug concentrations (Nokhodchi et al. 2012, Salouti and Ahangari 2014). Thus, our prepared nanoformulations with preserved antimicrobial efficiency can be a potential local drug delivery system for *the bone infection disease*, regardless of the exact *in vivo* mechanism. Designing of the sustained release antibiotic-loaded nanoparticles using a biodegradable and osteoconductive material such as $CaCO_3$ may be a promising expectation for bone infection therapy. Such a multipurpose carrier not only may reduce the costs of osteomyelitis therapy, but also it can decrease the treatment duration.

Conclusion

The treatment of chronic osteomyelitis involves removal of the infected bone along with antibiotic treatment. Systemic treatment of the osteomyelitis needs high serum concentrations of the antibiotics for the prolonged period of time, which leads to higher side effects. One of the most important advantages of novel drug delivery systems such as nanoparticles is to assure the effective therapy together with avoidance of toxicity by lowering the systemic blood levels of the antibiotics. In the present study, the prepared ciprofloxacin HCl-loaded $CaCO_3$ nanoparticles displayed appropriate physicochemical properties as well as a preserved antimicrobial effect against *S. aureus*, the *most* common microorganism involved in *osteomyelitis*. Local delivery of the ciprofloxacin HCl-loaded $CaCO_3$ nanoparticles through bone operation might have particular advantages, thanks to the great biocompatibility and osteoconductivity of the system. Such a sustained release antibiotic delivery system can provide a proper

situation for the growth of damaged bone with no need to an additional operation for the removal of the drug delivery system. Therefore, the prepared nanoparticles could be considered as a potential local drug delivery system for *osteomyelitis* in the future.

Acknowledgements

The authors would like to thank the Research Vice Chancellor of Tabriz University of Medical Sciences, for financial support of the study. This article is a part of a thesis (No. 96) submitted for the PhD degree in the Faculty of Pharmacy, Tabriz University of Medical Sciences.

Disclosure statement

The authors report no declarations of interest in this study.

References

Adams K, Couch L, Cierny G, Calhoun J, Mader JT. 1992. In vitro and in vivo evaluation of antibiotic diffusion from antibiotic-impregnated polymethylmethacrylate beads. Clin Orthopaed Rel Res. 278:244–252.

Adibkia K, Alaei-Beirami M, Barzegar-Jalali M, Mohammadi G, Ardestani MS. 2012. Evaluation and optimization of factors affecting novel diclofenac sodium-eudragit RS100 nanoparticles. Afr J Pharm Pharmacol. 6:941–947.

Adibkia K, Javadzadeh Y, Dastmalchi S, Mohammadi G, Niri FK, Alaei-Beirami M. 2011. Naproxen–Eudragit® RS100 nanoparticles: preparation and physicochemical characterization. Colloid Surf B: Biointer. 83:155–159.

Ahangari A, Salouti M, Heidari Z, Kazemizadeh AR, Safari AA. 2013. Development of gentamicin-gold nanospheres for antimicrobial drug delivery to Staphylococcal infected foci. Drug Deliv. 20:34–39.

Allahverdiyev AM, Kon KV, Abamor ES, Bagirova M, Rafailovich M. 2011. Coping with antibiotic resistance: combining nanoparticles with antibiotics and other antimicrobial agents. Expert Rev Anti Infect Ther. 9:1035–1052.

Andreassen J-P. 2005. Formation mechanism and morphology in precipitation of vaterite—nano-aggregation or crystal growth? J Crystal Grow. 274:256–264.

Barzegar-Jalali M. 1990. A model for linearizing drug dissolution data. Int J Pharm. 63:R9–R11.

Barzegar-Jalali M, Adibkia K, Valizadeh H, Shadbad MRS, Nokhodchi A, Omidi Y, et al. 2008. Kinetic analysis of drug release from nanoparticles. J Pharm Pharm Sci. 11:167–177.

Barzegar-Jalali M, Valizadeh H, Nazemiyeh H, Barzegar-Jalali A, Shadbad MRS, Adibkia K, Zare M. 2010. Reciprocal powered time model for release kinetic analysis of ibuprofen solid dispersions in oleaster powder, microcrystalline cellulose and crospovidone. J Pharma Pharm Sci. 13:152–161.

Benoit M-A, Mousset B, Delloye C, Bouillet R, Gillard J. 1998. Antibiotic-loaded plaster of Paris implants coated with poly lactide-co-glycolide as a controlled release delivery system for the treatment of bone infections. Int Orthopaed. 21:403–408.

Berne BJ, Pecora R. 2000. Dynamic Light Scattering: With Applications to Chemistry, Biology, and Physics. New York: John Wiley & Sons Publisher.

Biazar E, Heidari Keshel S, Tavirani MR, Jahandideh R. 2015. Bone reconstruction in rat calvarial defects by chitosan/hydroxyapatite nanoparticles scaffold loaded with unrestricted somatic stem cells. Artif Cells Nanomed Biotechnol. 43:112–116.

Beyssac E, Lavigne J. 2005. Dissolution study of active pharmaceutical ingredients using the flow through apparatus USP 4. Dissolut Technol. 12:23–25.

Blokhuis TJ, Termaat MF, Den Boer FC, Patka P, Bakker FC, Henk JTM. 2000. Properties of calcium phosphate ceramics in relation to their in vivo behavior. J Trauma Acute Care Surg. 48:179–186.

Brunton LL. 2011. Goodman & Gilman's the Pharmacological basis of therapeutics. New York: McGraw-Hill.

Cevher E, Orhan Z, Sensoy D, Ahiskali R, Kan PL, Sagirli O, Mülazimoglu L. 2007. Sodium fusidate-poly(D,L-lactide-co-glycolide) microspheres: preparation, characterisation and in vivo evaluation of their effectiveness in the treatment of chronic osteomyelitis. J Microencapsul. 24:577–595.

Chen J, Xiang L. 2009. Controllable synthesis of calcium carbonate polymorphs at different temperatures. Powder Technol. 189:64–69.

Clogston JD, Patri AK. 2011. Zeta potential measurement. Method Mol Biol. 697:63–70.

Cooper J, Hunt J. 2006. The significance of zeta potential in osteogenesis. Annual Meeting in conjunction with the 25th International Biomaterials Symposium. p. 592.

Darvishi B, Manoochehri S, Kamalinia G, Mostafavi SH, Maghazei S, Samadi N, et al. 2014. Preparation and antibacterial activity evaluation of 18-β-glycyrrhetinic acid loaded PLGA nanoparticles. Iran J Pharm Res. 14:373–383.

Dillen K, Vandervoort J, Van Den Mooter G, Ludwig A. 2006. Evaluation of ciprofloxacin-loaded Eudragit RS100 or RL100/PLGA nanoparticles. Int J Pharm. 314:72–82.

Dillen K, Vandervoort J, Van Den Mooter G, Verheyden L, Ludwig A. 2004. Factorial design, physicochemical characterisation and activity of ciprofloxacin-PLGA nanoparticles. Int J Pharms. 275:171–187.

Dizaj SM, Barzegar-Jalali M, Zarrintan MH, Adibkia K, Lotfipour F. 2015a. Calcium carbonate nanoparticles as cancer drug delivery system. Exp Opin Drug Deliv. 12:1649–1660.

Dizaj SM, Lotfipour F, Barzegar-Jalali M, Zarrintan M-H, Adibkia K. 2015b. Application of Box–Behnken design to prepare gentamicin-loaded calcium carbonate nanoparticles. Artif Cells Nanomed Biotechnol. [Epub ahead of print]. doi: 10.3109/21691401.2015.1042108.

Dizaj SM, Lotfipour F, Barzegar-Jalali M, Zarrintan MH, Adibkia K. 2014. Antimicrobial activity of the metals and metal oxide nanoparticles. Mater Sci Eng C Mater Biol Appl. 44:278–284.

Dizaj SM, Mennati A, Jafari S, Khezri K, Adibkia K. 2015c. Antimicrobial activity of carbon-based nanoparticles. Adv Pharm Bull. 5:19–23.

Drlica K, Zhao X. 1997. DNA gyrase, topoisomerase IV, and the 4-quinolones. Microbiol Mol Biol Rev. 61:377–392.

Eğri S, Eczacıoğlu N. 2016. Sequential VEGF and BMP-2 releasing PLA-PEG-PLA scaffolds for bone tissue engineering: I. Design and in vitro tests. Artif Cells Nanomed Biotechnol. [Epub ahead of print]. doi: 10.3109/21691401.2016.1147454.

Esmaeili F, Hosseini-Nasr M, Rad-Malekshahi M, Samadi N, Atyabi F, Dinarvand R. 2007. Preparation and antibacterial activity evaluation of rifampicin-loaded poly lactide-co-glycolide nanoparticles. Nanomed Nanotechnol Biol Med. 3:161–167.

Giamarellos-Bourboulis EJ. 2000. Carrier systems for the local delivery of antibiotics in bone infections. Drugs. 59:1223–1232.

Gürsel I, Korkusuz F, Türesin F, Gürdal Alaeddinoğlu N, Hasırcı V. 2000. In vivo application of biodegradable controlled antibiotic release systems for the treatment of implant-related osteomyelitis. Biomaterials. 22:73–80.

Haruta S, Hanafusa T, Fukase H, Miyajima H, Oki T. 2003. An effective absorption behavior of insulin for diabetic treatment following intranasal delivery using porous spherical calcium carbonate in monkeys and healthy human volunteers. Diabet Technol Therapeut. 5:1–9.

Honary S, Jahanshahi M, Golbayani P, Ebrahimi P, Ghajar K. 2010. Doxorubicin-loaded albumin nanoparticles: formulation and characterization. J Nanosci Nanotechnol. 10:7752–7757.

Honary S, Zahir F. 2013. Effect of zeta potential on the properties of nano-drug delivery systems-a review (Part 2). Trop J Pharm Res. 12:265–273.

Jahangiri A, Davaran S, Fayyazi B, Tanhaei A, Payab S, Adibkia K. 2014. Application of electrospraying as a one-step method for the fabrication of triamcinolone acetonide-PLGA nanofibers and nanobeads. Colloids Surf B Biointerfaces. 123:219–224.

Jain SK, Prajapati N, Rajpoot K, Kumar A. 2015. A novel sustained release drug–resin complex-based microbeads of ciprofloxacin HCl. Artif Cells Nanomed Biotechnol. [Epub ahead of print]. doi: 10.3109/21691401.2015.1111233.

Jana U, Mohanty AK, Pal SL, Manna PK, Mohanta GP. 2014. Felodipine loaded PLGA nanoparticles: preparation, physicochemical characterization and in vivo toxicity study. Nano Convergence. 1:1–10.

Jeong Y-I, Na H-S, Seo D-H, Kim D-G, Lee H-C, Jang M-K, et al. 2008. Ciprofloxacin-encapsulated poly(DL-lactide-co-glycolide) nanoparticles and its antibacterial activity. Int J Pharm. 352:317–323.

Kadivar A, Kamalidehghan B, Javar HA, Davoudi ET, Zaharuddin ND, Sabeti B, Chung LY, Noordin MI. 2015. Formulation and in vitro, in vivo evaluation of effervescent floating sustained-release imatinib mesylate tablet. PLoS One. 10:e0126874.

Kalam M, Humayun M, Parvez N, Yadav S, Garg A, Amin S, Sultana Y, Ali A. 2007. Release kinetics of modified pharmaceutical dosage forms: a review. Cont J Pharm Sci. 1:30–35.

Kamba SA, Ismail M, Hussein-Al-Ali SH, Ibrahim TT, Zakaria ZB. 2013. In vitro delivery and controlled release of doxorubicin for targeting osteosarcoma bone cancer. Molecules. 18:10580–10598.

Kesavan K, Nath G, Pandit J. 2010. Preparation and in vitro antibacterial evaluation of gatifloxacin mucoadhesive gellan system. DARU. 18:237.

Kirboga S, Oner M. 2013. Effect of the experimental parameters on calcium carbonate precipitation. Chem Eng. 32:2119–2124.

Koort J, Suokas E, Veiranto M. 2006. In vitro and in vivo testing of bioabsorbable antibiotic containing bone filler for osteomyelitis treatment. J Biomed Mater Res A. 78:532–540.

Korkusuz F, Korkusuz P, Ekşioğlu F, Gürsel İ, Hasırcı V. 2001. In vivo response to biodegradable controlled antibiotic release systems. J Biomed Mater Res. 55:217–228.

Kumar G, Sharma S, Shafiq N, Khuller GK, Malhotra S. 2012. Optimization, in vitro–in vivo evaluation, and short-term tolerability of novel levofloxacin-loaded PLGA nanoparticle formulation. J Pharm Sci. 101:2165–2176.

Lucas A, Gaudé J, Carel C, Michel J-F, Cathelineau G. 2001. A synthetic aragonite-based ceramic as a bone graft substitute and substrate for antibiotics. Int J Inorgan Mater. 3:87–94.

Mo Y, Lim L-Y. 2005. Paclitaxel-loaded PLGA nanoparticles: potentiation of anticancer activity by surface conjugation with wheat germ agglutinin. J Control Release. 108:244–262.

Mobarak DH, Salah S, Elkheshen SA. 2014. Formulation of ciprofloxacin hydrochloride loaded biodegradable nanoparticles: optimization of technique and process variables. Pharm Dev Technol. 19:891–900.

Montaseri H, Sayyafan M, Tajerzadeh H. 2010. Preparation and characterization of poly-(methyl ethyl cyanoacrylate) particles containing 5-aminosalicylic acid. Iran J Pharm Res. 1:21–27.

Neut D, Van De Belt H, Van Horn JR, Van Der Mei HC, Busscher HJ. 2003. Residual gentamicin-release from antibiotic-loaded polymethylmethacrylate beads after 5 years of implantation. Biomaterials. 24:1829–1831.

Ni M, Ratner BD. 2008. Differentiating calcium carbonate polymorphs by surface analysis techniques—an XPS and TOF-SIMS study. Surf Int Anal. 40:1356–1361.

Nokhodchi A, Mohammadi G, Ghafourian T. 2012. Nanotechnology Tools for Efficient Antibacterial Delivery to Salmonella. New York: InTech Open Access Publisher.

Ofoefule S, Chukwu A. 2002. Sustained release dosage forms: design and evaluation of oral products. In: Ofoefule SI, Ed. Textbook of Pharmaceutical Technology and Industrial Pharmacy. Lagos, Nigeria: Samakin (Nig.) Enterprises, pp. 94–120.

Perry CR, Rice S, Ritterbusch JK, Burdge RE. 1985. Local administration of antibiotics with an implantable osmotic pump. Clin Orthopaedic Relat Res. 192:284–290.

Qian K, Shi T, Tang T, Zhang S, Liu X, Cao Y. 2011. Preparation and characterization of nano-sized calcium carbonate as controlled release pesticide carrier for validamycin against *Rhizoctonia solani*. Microchim Acta. 173:51–57.

Sah E, Sah H. 2015. Recent trends in preparation of poly(lactide-co-glycolide) nanoparticles by mixing polymeric organic solution with antisolvent. J Nanomater. 2015:1–22.

Sahoo S, Chakraborti CK, Mishra SC. 2011. Qualitative analysis of controlled release ciprofloxacin/carbopol 934 mucoadhesive suspension. J Adv Pharm Technol Res. 2:195–204.

Salouti M, Ahangari A. 2014. Nanoparticle Based Drug Delivery Systems for Treatment of Infectious Diseases. New York: InTech.

Shen Y, Xie A, Chen Z, Xu W, Yao H, Li S, et al. 2007. Controlled synthesis of calcium carbonate nanocrystals with multi-morphologies in different bicontinuous microemulsions. Mater Sci Eng: A. 443:95–100.

Silverstein RM, Webster FX, Kiemle D, Bryce DL. 2014. Spectrometric Identification of Organic Compounds. New York: John Wiley & Sons.

Smeets R, Kolk A, Gerressen M, Driemel O, Maciejewski O, Hermanns-Sachweh B, et al. 2009. A new biphasic osteoinductive calcium composite material with a negative Zeta potential for bone augmentation. Head Face Med. 5:13.

Solberg BD, Gutow AP, Baumgaertner MR. 1999. Efficacy of gentamycin-impregnated resorbable hydroxyapatite cement in treating osteomyelitis in a rat model. J Orthopaed Trauma. 13:102–106.

Tai CY, Chen C-K. 2008. Particle morphology, habit, and size control of $CaCO_3$ using reverse microemulsion technique. Chem Eng Sci. 63:3632–3642.

Teng N, Nakamura S, Takagi Y, Yamashita Y, Ohgaki M, Yamashita K. 2001. A new approach to enhancement of bone formation by electrically polarized hydroxyapatite. J Dent Res. 80:1925–1929.

Ueno Y, Futagawa H, Takagi Y, Ueno A, Mizushima Y. 2005. Drug-incorporating calcium carbonate nanoparticles for a new delivery system. J Control Release. 103:93–98.

Ukrainczyk M, Kontrec J, Babić-Ivančić V, Brečević L, Kralj D. 2007. Experimental design approach to calcium carbonate precipitation in a semicontinuous process. Powder Technol. 171:192–199.

Ukrainczyk M, Kontrec J, Kralj D. 2009. Precipitation of different calcite crystal morphologies in the presence of sodium stearate. J Colloid Interface Sci. 329:89–96.

Uskoković V, Desai TA. 2014. Simultaneous bactericidal and osteogenic effect of nanoparticulate calcium phosphate powders loaded with clindamycin on osteoblasts infected with *Staphylococcus aureus*. Mater Sci Eng C. 37:210–222.

Vogelman B, Gudmundsson S, Leggett J, Turnidge J, Ebert S, Craig W. 1988. Correlation of antimicrobial pharmacokinetic parameters with therapeutic efficacy in an animal model. J Infect Dis. 158:831–847.

Waldvogel FA, Medoff G, Swartz MN. 1970. Osteomyelitis: a review of clinical features, therapeutic considerations and unusual aspects. N Eng J Med. 282:316.

Wang Y, Moo YX, Chen C, Gunawan P, Xu R. 2010. Fast precipitation of uniform $CaCO_3$ nanospheres and their transformation to hollow hydroxyapatite nanospheres. J Colloid Interface Sci. 352:393–400.

Zhang L, Pornpattananangkul D, Hu C-M, Huang C-M. 2010. Development of nanoparticles for antimicrobial drug delivery. Curr Med Chem. 17:585–594.